Modeling and Simulation of a Biomimetic Underwater Vehicle

Tiago G. António[1] Paulo P. Silva[1] Bruno Damas[1,2] Miguel B. Moreira[1]

goncalves.antonio@marinha.pt, {pires.silva,bruno.damas,miguel.moreira}@escolanaval.pt

***Abstract*—This paper describes the mathematical model developed to simulate the behavior of a BUV, the TOBIAS vehicle, which is being developed at the Portuguese Naval Academy as part of the SABUVIS project. During the development of the model the hydrodynamic coefficients of the vehicle were estimated, as well as the thrust generated by the undulatory motion of the tail and the effects of the pectoral fins. Using this model, it is possible to perform a series of maneuvers verifying the performance of the BUV as a function of different control parameters.**

***Keywords*—Biomimetic Underwater Vehicle, Modeling, Undulating Propulsion, Simulation**

I. Introduction

The significant development in the area of underwater robotics has led to the emergence of several models of Autonomous Underwater Vehicles (AUV), engaging them in military, scientific, or commercial missions, performing tasks such as mine countermeasures, examining oil and gas pipelines, or hydrographic surveys and mapping of the ocean floor [1]. However, it has been found that in certain situations these propelled AUVs are underperforming, due to their poor maneuverability at low speeds, resulting in a high radius of gyration. Therefore, other propulsion configurations such as azimuthal thrusters or multiple thrusters distributed along the vehicle body with different orientations have been adopted, at a cost of an increased energy consumption [1].

Thus, the need arose to develop a propulsion system that would ensure good maneuverability of the vehicle while guaranteeing its energy efficiency. For this purpose, nature was used as inspiration and the swimming modes of fish where mimicked, resulting in an efficient alternative propulsion system. So, the concept of the Biomimetic Underwater Vehicle (BUV) appears, where the thrusters are replaced by a tail that reproduces the undulatory movement similar to a fish [2]. The BUVs, in addition to solving the problem of energy efficiency combined with good maneuverability also have other advantages compared to propelled vehicles, namely the reduction of noise during their movement and their stealthiness, reducing the probability of being detected, which are relevant characteristics for military applications of these devices [3].

[1]CINAV - Centro de Investigação Naval, Portuguese Naval Academy, Almada, Portugal.

[2]Institute for Systems and Robotics, Instituto Superior Tecnico, Universidade de Lisboa, Portugal

The dynamic behaviour of a vehicle with undulating propulsion is more complex than the dynamics of vehicles with traditional propellers, and there has been a large research on modeling the dynamics of these kind of vehicles that mimic fish, stingrays and other type of aquatic creatures [4], [5]. In [6], computational fluid dynamic simulation is used to obtain an accurate prediction of the hydrodynamic forces applied on a robotic fish, while in [7] the dynamic equations of a BUV are derived and a method to find the optimal parameters to give a maximum propulsive power is proposed. [8], on the other hand, presents a dynamic model divided into a stiff anterior body, a flexible rear body, and an oscillating lunate caudal fin, using unsteady flow theory to analyze the motion of the anterior part and the links, and basic airfoil theory for the caudal fin. An approach based on a six degree-of-freedom multi-body model, that considers the BUV as comprised of multiple rigid bodies interlinked through joints, is presented in [9]. The hydrodynamics of swimming and undulating propulsion is thoroughly studied in [10], [11], while in [12], [13] the propulsive thrust of undulating propulsion is experimentally obtained.

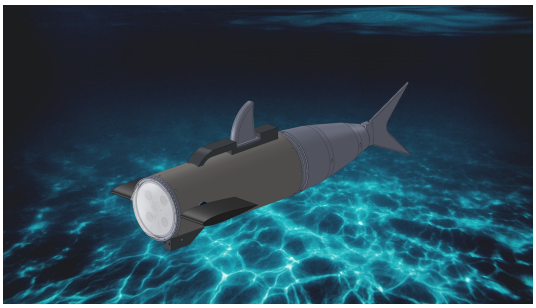

Fig. 1. BUV TOBIAS.

The BUV TOBIAS (Fig. 1) is a vehicle under development at the Portuguese Naval Academy, as part of the SABUVIS project, whose main goal is to develop a swarm of biomimetic vehicles with the ability to operate autonomously and perform tasks in a cooperative manner [3], [14]. This vehicle is inspired by fish, with carangiform swimming mode and has a tail with two joints controlled by servo-motors, which attempt to replicate the undulatory behavior of biological species. The BUV TOBIAS is also equipped with two pectoral fins with NACA0012 profile, whose variation in angle of attack allows for the control of the vehicle's attitude.

This paper main contribution is the derivation of the dynamical model of the BUV TOBIAS, based on the computational estimation of its hydrodynamic coefficients, as well as the thrust generated by the undulatory motion of the tail and the effects of the pectoral fins on the the vertical motion of the BUV. Simulation results are presented to validate the approach. This paper is structurally organized as follows: Section 2 briefly explains the mathematical model of the TOBIAS BUV; Section 3 describe the simulations performed, testing the performance of the model; and finally in Section 4 are discussed the conclusions of this work and also suggested some ideas for the future of the project.

II. TOBIAS Mathematical Model

The development and use of mathematical models to simulate the behavior of vehicles is a common practice, acting as a decision support tool throughout vehicle design and assembly. Thus, the modeling of the behavior of the BUV TOBIAS will be driven acording to the model presented by Fossen in [15], however, adapting it by adding or replacing terms, in order to represent the biomimetic nature of the vehicle.

Underwater vehicles have 6 Degrees Of Freedom (DOF) associated with translational and rotational movements about all three axes (Fig. 2). A common practice in this type of models is to adopt, by convenience, reference frames that allow, through reference points, to know the position, orientation and velocity of the vehicle [16]. Thus, Fossen considers two reference frames, one inertial fixed to the Earth and the other fixed to the vehicle body which moves with it [1], [15], as shown in Fig. 2.

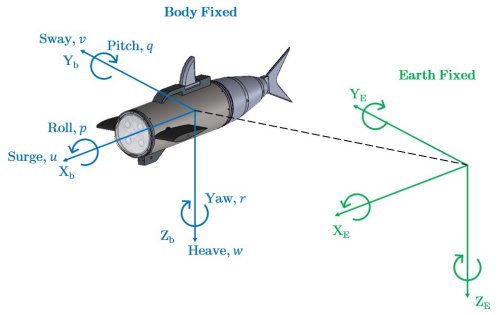

Fig. 2. Degrees of freedom and reference frames.

For the purpose of developing this model, the variables that describe the position, orientation, velocities, as well as the forces and moments acting on the vehicle are defined according to equation (1)

$$\begin{aligned} \eta &= \begin{bmatrix}\eta_1\\ \eta_2\end{bmatrix}; \quad \eta_1 = \begin{bmatrix}x\\ y\\ z\end{bmatrix}; \quad \eta_2 = \begin{bmatrix}\phi\\ \theta\\ \psi\end{bmatrix}; \\ \nu &= \begin{bmatrix}\nu_1\\ \nu_2\end{bmatrix}; \quad \nu_1 = \begin{bmatrix}u\\ v\\ w\end{bmatrix}; \quad \nu_2 = \begin{bmatrix}p\\ q\\ r\end{bmatrix}; \\ \tau &= \begin{bmatrix}\tau_1\\ \tau_2\end{bmatrix}; \quad \tau_1 = \begin{bmatrix}X\\ Y\\ Z\end{bmatrix}; \quad \tau_2 = \begin{bmatrix}K\\ M\\ N\end{bmatrix}; \end{aligned} \tag{1}$$

where η_1 and η_2, respectively, correspond to the position and orientation of the vehicle in the inertial reference frame fixed to the Earth; ν_1 and ν_2 are the linear and angular velocity vectors defined in the body fixed reference frame; τ_1 and τ_1 are the forces and moments acting on the vehicle, also expressed in the reference frame fixed to the body.

The model mentioned in [15] describes the behavior of the vehicle through its kinematics and dynamics, as presented in the following sections.

A. Vehicle Kinematics

As mentioned earlier, the vehicle velocities derived from the dynamic component of the movement are associated with the reference frame fixed to the body. Thus, to represent these velocities in the inertial reference frame fixed to the Earth, the Euler angles are used, establishing a geometrical relationship between both reference frames [15]. These relationships between the two reference frames are expressed through two transformation matrices J_1 and J_2, the first being applied to the linear velocities (ν_1) and the second to the angular velocities (ν_2), as shown in equation (2)

$$\begin{aligned} \dot{\eta}_1 &= J_1(\eta_2)\upsilon_1, \\ \dot{\eta}_2 &= J_2(\eta_2)\upsilon_2, \end{aligned} \tag{2}$$

the transformation matrices are defined according to equation (3), where c stands for cosine and s for sine

$$\begin{aligned} J_1(\eta_2) &= \begin{bmatrix} \mathrm{c}\psi\mathrm{c}\theta & -\mathrm{s}\psi\mathrm{c}\phi + \mathrm{c}\psi\mathrm{s}\theta\mathrm{s}\phi & \mathrm{s}\psi\mathrm{s}\phi + \mathrm{c}\psi\mathrm{c}\phi\mathrm{s}\theta \\ \mathrm{s}\psi\mathrm{c}\theta & \mathrm{c}\psi\mathrm{c}\phi + \mathrm{s}\phi\mathrm{s}\theta\mathrm{s}\psi & -\mathrm{c}\psi\mathrm{s}\phi + \mathrm{s}\theta\mathrm{s}\psi\mathrm{c}\phi \\ -\mathrm{s}\theta & \mathrm{c}\theta\mathrm{s}\phi & \mathrm{c}\theta\mathrm{c}\phi \end{bmatrix}; \\ J_2(\eta_2) &= \begin{bmatrix} 1 & \mathrm{s}\phi\mathrm{t}\theta & \mathrm{c}\phi\mathrm{t}\theta \\ 0 & \mathrm{c}\phi & -\mathrm{s}\phi \\ 0 & \mathrm{s}\phi/\mathrm{c}\theta & \mathrm{c}\phi/\mathrm{c}\theta \end{bmatrix}. \end{aligned} \tag{3}$$

B. Vehicle Dynamics

The dynamic behavior of the BUV TOBIAS in the 6 DOF is mathematically modeled, with respect to the reference frame fixed on the vehicle body, through equation (4) [15]

$$M\dot{\nu} + C(\nu)\nu + D(\nu)\nu + g(\eta) = \tau, \tag{4}$$

where M represents the mass and inertia matrix (including added mass), $C(\nu)$ is the matrix of Coriolis and centripetal terms (also including the effect of added mass), $D(\nu)$ corresponds to the damping matrix, $g(\eta)$ is the vector of restoring forces and moments, and τ represents the vector of forces and moments produced by the tail and pectoral fins as a result of the different control parameters [1].

A number of assumptions will be considered on a first approach to modeling the dynamic behavior of the BUV TOBIAS as a way to simplify the process. The vehicle is assumed to have neutral buoyancy, with its Center of Gravity (CG) at the origin of the reference frame fixed to the body, $r_g = [0 \quad 0 \quad 0]^T$, and the Center of Buoyancy (CB) slightly above the previous, $r_b = [0 \quad 0 \quad z_b]^T$.

The added mass terms due to the movement of the vehicle in the water, are obtained by approximating the body of the BUV TOBIAS to a prolate ellipsoid. Thus, due to the symmetry of

the ellipsoid, the added mass derivatives are reduced to the diagonal terms [17], calculated according to equation (5),

$$\begin{aligned} X_{\dot{u}} &= \frac{\alpha_0}{2-\alpha_0} m, \\ Y_{\dot{v}} = Z_{\dot{w}} &= \frac{\beta_0}{2-\beta_0} m, \\ K_{\dot{p}} &= 0, \\ N_{\dot{r}} = M_{\dot{q}} &= \frac{1}{5} \frac{\left(b^2-a^2\right)^2 (\alpha_0 - \beta_0)}{2\left(b^2-a^2\right) + \left(b^2+a^2\right)(\beta_0 - \alpha_0)} m, \end{aligned} \tag{5}$$

where m corresponds to the vehicle mass, a and b to the major and minor radius of the ellipsoid, α_0 and β_0 are defined according to equation (6)

$$\begin{aligned} \alpha_0 &= \frac{2\left(1-e^2\right)}{e^3}\left(\frac{1}{2}\ln\frac{1+e}{1-e} - e\right), \\ \beta_0 &= \frac{1}{e^2} - \frac{1-e^2}{2e^3}\ln\frac{1+e}{1-e}, \\ e &= 1 - \left(\frac{b}{a}\right)^2. \end{aligned} \tag{6}$$

Therefore, the mass and inertia matrix (M) and the Coriolis and centripetal terms matrix ($C(\nu)$) are defined according to equations (7) and (8), respectively, including in addition to the rigid body properties, the added mass derivatives.

$$M = \begin{bmatrix} m - X_{\dot{u}} & 0 & 0 & 0 & 0 & 0 \\ 0 & m - Y_{\dot{v}} & 0 & 0 & 0 & 0 \\ 0 & 0 & m - Z_{\dot{w}} & 0 & 0 & 0 \\ 0 & 0 & 0 & I_x - K_{\dot{p}} & -I_{xy} & -I_{xz} \\ 0 & 0 & 0 & -I_{yx} & I_y - M_{\dot{q}} & -I_{yz} \\ 0 & 0 & 0 & -I_{zx} & -I_{zy} & I_z - N_{\dot{r}} \end{bmatrix} \tag{7}$$

$$C(\nu) = \begin{bmatrix} 0 & 0 & 0 \\ 0 & 0 & 0 \\ 0 & 0 & 0 \\ 0 & w(m - Z_{\dot{w}}) & v(Y_{\dot{v}} - m) \\ w(Z_{\dot{w}} - m) & 0 & u(m - X_{\dot{u}}) \\ v(m - Y_{\dot{v}}) & u(X_{\dot{u}} - m) & 0 \end{bmatrix}$$

$$\begin{bmatrix} 0 & w(m - Z_{\dot{w}}) & v(Y_{\dot{v}} - m) \\ w(Z_{\dot{w}} - m) & 0 & u(m - X_{\dot{u}}) \\ v(m - Y_{\dot{v}}) & u(X_{\dot{u}} - m) & 0 \\ 0 & -I_{yz}q - I_{xz}p + r(I_z - N_{\dot{r}}) & I_{yz}r + I_{xy}p + q(M_{\dot{q}} - I_y) \\ I_{yz}q + I_{xz}p + r(N_{\dot{r}} - I_z) & 0 & -I_{xz}r - I_{xy}q + p(I_x - K_{\dot{p}}) \\ -I_{yz}r - I_{xy}p + q(I_y - M_{\dot{q}}) & I_{xz}r + I_{xy}q + p(K_{\dot{p}} - I_x) & 0 \end{bmatrix} \tag{8}$$

In an early stage of modeling the BUV TOBIAS, only quadratic damping will be considered [18], which is mathematically defined by the equation (9),

$$D = -\frac{1}{2}\rho C_D A |U| U, \tag{9}$$

where ρ is the water density, C_D is the drag coefficient that varies with Reynolds number and body geometry, A is the cross-sectional area and U is the vehicle velocity. This equation is not only used to calculate the drag force acting in surge, sway and heave, but also to estimate the rotational drag terms in roll, pitch, and yaw [1], [18].

Although previously the BUV TOBIAS has been approximated to a prolate ellipsoid, it has fins (pectoral, dorsal and caudal) and appendices that generate significant drag at certain DOFs. Thus, to obtain the drag coefficients of the different components, rough approximations are made to simpler structures with known values. The dorsal fin and appendices are approximated to a flat plate $C_D \approx 1.2$ [19]. The caudal fin is approximated to a wedge $C_D \approx 0.5$, considering, at first, only its initial position aligned with the body [1], [19]. The pectoral fins will be discussed later. The drag coefficient of the main body is obtained by approximating it to a prolate ellipsoid, getting $C_D \approx 0.2$ [1], [19]. Considering the fins and appendices of the BUV TOBIAS, it has only one plane of symmetry formed by the axes $\{X_b, Z_b\}$, so the damping matrix ($D(\nu)$) will be defined according to equation (10), with the terms estimated through equation (9) [16].

$$D(\nu) = -\begin{bmatrix} X_{u|u|}|u| & 0 & 0 & 0 & X_{q|q|}|q| & 0 \\ 0 & Y_{v|v|}|v| & 0 & Y_{p|p|}|p| & 0 & Y_{r|r|}|r| \\ 0 & 0 & Z_{w|w|}|w| & 0 & Z_{q|q|}|q| & 0 \\ 0 & K_{v|v|}|v| & 0 & K_{p|p|}|p| & 0 & 0 \\ M_{u|u|}|u| & 0 & M_{w|w|}|w| & 0 & M_{q|q|}|q| & 0 \\ 0 & N_{v|v|}|v| & 0 & 0 & 0 & N_{r|r|}|r| \end{bmatrix} \tag{10}$$

Due to the previously mentioned assumptions concerning the neutral buoyancy of the vehicle and the positions of CG and CB, the restoring forces and moments caused by the Weight (W) and Buoyancy (B) are described through equation (11)

$$g(\eta) = \begin{bmatrix} 0 \\ 0 \\ 0 \\ (-z_b B)\cos\theta\sin\phi \\ (-z_b B)\sin\theta \\ 0 \end{bmatrix}. \tag{11}$$

C. Pectoral Fins

The BUV TOBIAS has two pectoral fins, with the known profile NACA0012, which produce an effect that is similar to an aircraft's wings, where Lift (L) and Drag (D) forces are function of the angle of attack (α) [2], [20]. These forces are mathematically approximated by

$$L = \frac{1}{2}\rho A u^2 C_L \qquad \text{and} \qquad D = \frac{1}{2}\rho A u^2 C_D, \tag{12}$$

where A is the cross-sectional area of the fin, u is the water flow velocity (assumed to be equal to the surge velocity), C_L and C_D are the lift and drag coefficients which vary their values depending on α.

Therefore, considering the location of the pectoral fins on both sides, Port (P) and Starboard (S), relative to the CG of the vehicle (Fig. 3), the forces and moments associated with each one of them are described in equation (13).

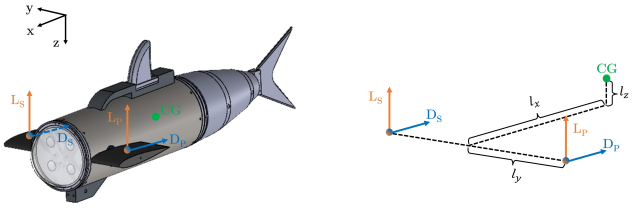

Fig. 3. Forces acting on the pectoral fins.

$$\tau_{PF} = \begin{bmatrix} -D_P - D_S \\ 0 \\ -L_P - L_S \\ L_P l_y - L_S l_y \\ L_P l_x - D_P l_z + L_S l_x - D_S l_z \\ -D_P l_y + D_S l_y \end{bmatrix} \tag{13}$$

D. Biomimetic propulsion system

The biomimetic propulsion system of the BUV TOBIAS (Fig. 4) consists of two servo motors, mounted on the support bases, which transmit motion to their associated plates. The plates are coupled to rods attached to the ribs of the vehicle, thus generating the undulating movement of the tail.

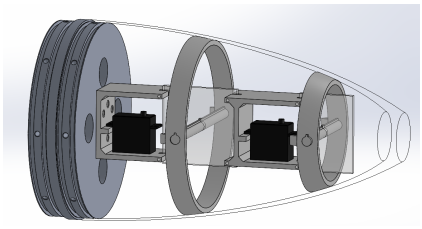

Fig. 4. The biomimetic propulsion system.

The tail mechanism is modelled by considering 2 revolute joints, as being the articulations of the biomimetic propulsion system. Thus, through this simplification, the system can be modeled as a robot manipulator, using the Denavit-Hartenberg (D-H) representation to describe the tail kinematics [1], [2], [21]. The D-H representation consists of assigning to each joint a reference frame, according to a set of rules and procedures [21], as shown in Fig. 5.

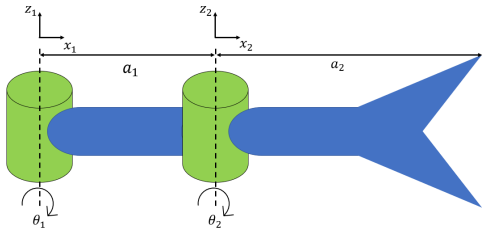

Fig. 5. D-H representation of the tail with 2 revolute joints.

Using this representation, it is possible to estimate the kinematics of the biomimetic propulsion mechanism, verifying parameters such as the lateral displacement of the caudal fin in relation to the first joint [2], which corresponds to the first servo motor attached to the vehicle body. As a way of showing the usefulness of this representation, Fig. 6 presents the kinematics of this mechanism in four different oscillation positions, with the first two points corresponding to the position of the servo motors and the last one corresponding to the tail tip. The distances between the points correspond to the lengths a_1 and a_2 mentioned in Fig. 5.

The thrust generated by the undulatory motion of the tail will be estimated using the Lighthill's Large Amplitude

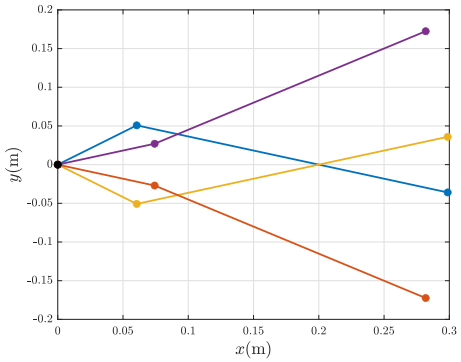

Fig. 6. Simulated tail kinematics.

Elongated Body Theory [22], [23]. This approach concentrates on the end of the caudal fin, as this is the point with the largest lateral displacement (and therefore the greatest impact on the water), and it considers that the total rate of change of momentum results from the sum of three components: (i) the rate of change of momentum that is left behind at the end of the tail blade, (ii) the rate of change of momentum due to pressure differences between the part of the water around the fish and the wake behind the fish, (iii) the reactive force F_{Prop} propelling the fish forward [23]. Thus, the thrust force (F_{Prop}) produced due to the periodic undulatory motion of the tail is expressed by equation (14)

$$F_{Prop} = \left(mwk \sin\theta + \frac{1}{2} mw^2 \cos\theta \right)_{tail}, \tag{14}$$

where m is the added mass of the tail per unit length, θ is the angle between the tail surface and the swimming direction x, k and w are the tangential and perpendicular components of the instantaneous velocity vector of the tail tip, as shown in Fig. 7.

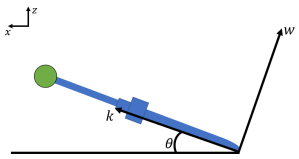

Fig. 7. Diagram from the 2^{nd} servo motor to the tail tip.

These components of the instantaneous velocity vector of the tail tip are mathematically defined by equation (15)

$$\begin{aligned} k &= \frac{dz}{dt} \sin\theta + \frac{dx}{dt} \cos\theta, \\ w &= \frac{dz}{dt} \cos\theta - \frac{dx}{dt} \sin\theta. \end{aligned} \tag{15}$$

The θ angle results, as seen in Fig. 6, from the combined actuation of both servo motors. In an initial approach to modeling the BUV TOBIAS, it is assumed that they produce, at the tail tip, a sinusoidal oscillation behavior that is mathematically defined by equation (16)

$$\theta(t) = \theta_A \sin(2\pi f t), \tag{16}$$

where θ_A and f are control parameters of the biomimetic propulsion, defining, respectively, the oscillation amplitude and frequency of the tail tip.

That said, taking into account the trigonometric relationships presented in Fig. 7, the derivatives $\frac{dx}{dt}$ and $\frac{dz}{dt}$ mentioned in equation (15), can be roughly approximated by equation (17)

$$\begin{aligned} \frac{dx}{dt} &= \frac{d(a_2 \cos\theta)}{dt} = -a_2 \sin\theta \frac{d\theta}{dt}, \\ \frac{dz}{dt} &= \frac{d(a_2 \sin\theta)}{dt} = a_2 \cos\theta \frac{d\theta}{dt}, \end{aligned} \tag{17}$$

where a_2 is the length of the 2^{nd} link (Fig. 5).

Another biomimetic propulsion control parameter is the Tail Deflection Angle (θ_{TDA}), which consists of the angle between the vehicle centerline and the tail oscillation centerline [1]. Thus, the maneuvering of the BUV TOBIAS in the horizontal plane is accomplished by changing this parameter, which consequently changes the direction of the generated thrust force, as shown in Fig. 8.

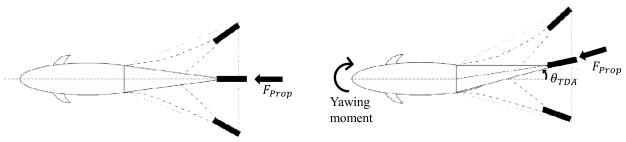

Fig. 8. Maneuvering through changing the angle θ_{TDA}.

Therefore, the forces and moments produced by the biomimetic propulsion system are defined according to equation (18) [1]

$$\tau_{Prop} = \begin{bmatrix} F_{Prop} \cos(\theta_{TDA}) \\ F_{Prop} \sin(\theta_{TDA}) \\ 0 \\ 0 \\ 0 \\ (F_{Prop} \sin(\theta_{TDA}))\, l_{CG} \end{bmatrix}, \tag{18}$$

where l_{CG} is the perpendicular distance between the tail tip and the CG. The recoil motions expressed through roll and yaw moments will be neglected, assuming that tail mass represents a small portion of the total mass of the vehicle and that the cross-sectional area of the vehicle is large enough [1], [22].

III. Numerical Simulation

To verify the performance of the developed model, 3 basic maneuvers will be simulated: forward swimming, turning circle, dive and emersion.

A. Forward Swimming

It is shown in Fig. 9 the simulation results of the forward swimming, for various oscillation frequencies while keeping the amplitude equivalent to 10% of the vehicle length [23], implying roughly that $\theta_A = 27°$. This shows the effect of increasing the oscillation frequency on the surge velocity, and it also indicates that the average values in each configuration

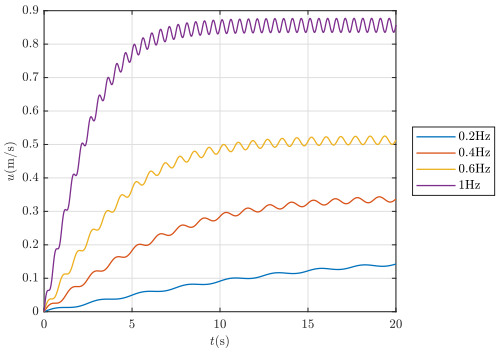

Fig. 9. Simulated forward swimming - surge velocity.

are slightly below the expected for a real fish [23], however this result would be expected as the vehicle, unlike a fish, has a rigid body [2].

B. Turning Circle

Fig. 10 shows the simulation results of the turning circle maneuver, while keeping the oscillation frequency and amplitude at 1Hz and 20°, and varying the tail deflection angle. The BUV initializes the movement by performing the forward swimming, stabilizing the surge velocity, and after that, at the instant indicated by the black star, it begins the maneuver by varying the parameter θ_{TDA}. This shows the rudder effect

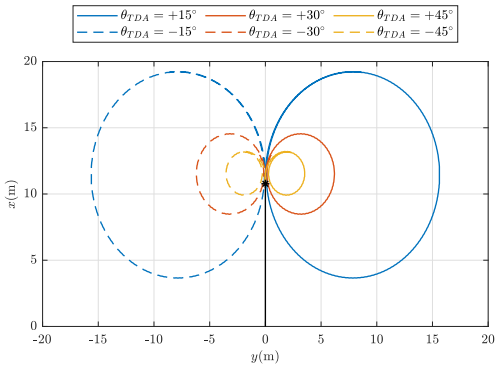

Fig. 10. Simulated turning circle.

produced by the tail deflection, verifying that the vehicle turns to starboard if $\theta_{TDA} > 0$ and to port otherwise. Furthermore, this simulation also shows, as expected, that the larger the θ_{TDA} the smaller the tactical diameter will be, obtaining values of 15.6m, 6.1m and 3.5m, respectively.

C. Dive and Emersion

Shown in Fig. 11 are the simulation results for dive and emersion, while keeping the parameters f, θ_A and θ_{TDA} constant throughout the maneuver with the values, 1Hz, 20° and 0°, respectively. The vehicle starts the simulation by performing a forward swimming, stabilizing the surge velocity, and after that, at the instant indicated by the black star, the pectoral fins on both sides (Port (P) and Starboard (S)) are actuated, varying their angle of attack. This figure shows the

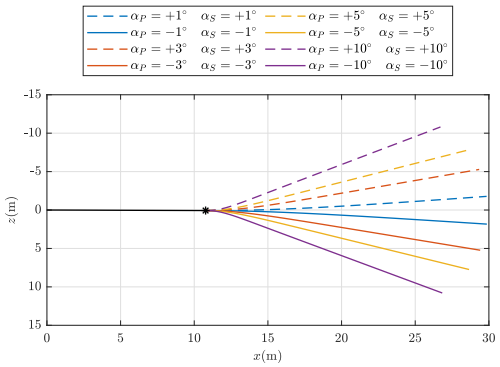

Fig. 11. Simulated dive and emersion.

effect produced by the pectoral fins, causing the BUV to dive when $\alpha < 0°$ and ascend otherwise, also showing that the depth change is proportional to the increase in the angle of attack. The reason for this is due to the C_L provided in the NACA0012 data sheet, since for each angle of attack set, it affects the direction and magnitude of the lift force, causing the vehicle to vary its depth.

The depth variations, while diving and emerging, occur in an approximately symmetrical way, for the same actuation, in absolute value, of the pectoral fins. This occurs because the pectoral fins that equip the BUV TOBIAS have a symmetrical profile in relation to its horizontal plane, which also causes symmetrical lift coefficients.

IV. Conclusion

This paper presents an initial, and simple approach, to developing a mathematical model to describe the behavior of the biomimetic vehicle TOBIAS. The vehicle has an articulated tail, with two servo motors, that attempts to replicate the undulatory motion similar to a fish, and in order to control its motion it is also equipped with a pectoral fin on each side. The actuation of these servo motors and the pectoral fins allows testing different configurations of propulsion and maneuvering, verifying the vehicle's performance in a wide range of situations, being however aware of the physical operational limits of these actuators.

During the development of the mathematical model some assumptions were considered, in order to simplify the modelling process, namely in obtaining the hydrodynamic coefficients of the vehicle, where it was roughly approximated to simpler geometric shapes, and in the estimation of the thrust force generated by the undulatory motion of the tail where only the events occurring at its tip were taken into account.

The performance of the model under the different simulated maneuvers occurs as physically expected. However, due to the assumptions previously mentioned and others described throughout the paper, these results have a slight degree of uncertainty. That said, there is room for improvement, suggesting as future work, after the BUV TOBIAS construction is completed, the experimental validation of this model, as well as determining the hydrodynamic coefficients of the vehicle in a test tank. After this validation and tuning of the model, control algorithms can be developed to simulate and test more complex maneuvers. In addition, by taking into account and including environmental events, such as ocean currents and waves, it will be possible to increase the realism of the model, producing more reliable simulations.

References

[1] A. N. A. Mazlan, "A Fully Actuated Tail Propulsion System for a Biomimetic Autonomous Underwater Vehicle," 2015.

[2] C. M. Watts, "A Comparison Study of Biologically Inspired Propulsion Systems for An Autonomous Underwater Vehicle," pp. 175–178, 2009.

[3] J. G. D. Paiva, "Desenvolvimento de um Veículo Autónomo Biomimético," Master's thesis, Escola Naval, 2020.

[4] J. Liu and H. Hu, "Biological inspiration: From carangiform fish to multi-joint robotic fish," *Journal of Bionic Engineering*, vol. 7, no. 1, pp. 35–48, mar 2010.

[5] R. Salazar, A. Campos, V. Fuentes, and A. Abdelkefi, "A review on the modeling, materials, and actuators of aquatic unmanned vehicles," *Ocean Engineering*, vol. 172, pp. 257–285, 2019.

[6] Z. Guan, W. Gao, N. Gu, and S. Nahavandi, "3D hydrodynamic analysis of a biomimetic robot fish," *11th International Conference on Control, Automation, Robotics and Vision, ICARCV 2010*, no. December, pp. 793–798, 2010.

[7] H. S. Kim, B. R. Lee, and R. J. Kim, "A study on the motion mechanism of articulated fish robot," *Proc. of the IEEE International Conference on Mechatronics and Automation, ICMA 2007*, pp. 485–490, 2007.

[8] J. Yu, L. Liu, and L. Wang, "Dynamic modeling and experimental validation of biomimetic robotic fish," *Proceedings of the American Control Conference*, vol. 2006, pp. 4129–4134, 2006.

[9] P. Krishnamurthy, F. Khorrami, J. De Leeuw, M. E. Porter, K. Livingston, and J. H. Long, "A multi-body approach for 6DOF modeling of biomimetic autonomous underwater vehicles with simulation and experimental results," *Proceedings of the IEEE International Conference on Control Applications*, pp. 1282–1287, 2009.

[10] M. Bozkurttas, J. Tangorra, G. Lauder, and R. Mittal, "Understanding the hydrodynamics of swimming: From fish fins to flexible propulsors for autonomous underwater vehicles," *CIMTEC 2008 - Proceedings of the 3rd International Conference on Smart Materials, Structures and Systems - Mining Smartness from Nature*, vol. 58, pp. 193–202, 2008.

[11] X. Yin, L. Jia, C. Wang, and G. Xie, "Modelling of thrust generated by oscillation caudal fin of underwater bionic robot," *Applied Mathematics and Mechanics (English Edition)*, vol. 37, no. 5, pp. 601–610, 2016.

[12] V. Powers, C., Mellinger, D., Kushleyev, A., Kothmann, B., Kumar, *Design, Modeling, and Characterization of a Miniature Robotic Fish for Research and Education in Biomimetics and Bioinspiration*. IEEE, 2013, vol. 18, no. 287513.

[13] P. Szymak, "Mathematical model of underwater vehicle with undulating propulsion," in *3rd International Conf. on Mathematics and Computers in Sciences and in Industry (MCSI)*. IEEE, 2016, pp. 269–274.

[14] H. F. R. Araújo, "Projeto e desenvolvimento de um veículo autónomo biomimético de subsuperfície," Master's thesis, Escola Naval, 2020.

[15] T. I. Fossen, *Handbook of Marine Craft Hydrodynamics and Motion Control*. John Wiley & Sons, Ltd, apr 2011.

[16] B. Ferreira, "Modelação e controlo de veículo submarino com quatro graus de liberdade," Master's thesis, FEUP, 2009.

[17] T. I. Fossen, *Guidance and Control of Ocean Vehicles*. John Wiley & Sons, Ltd, 1994.

[18] S. C. Tang, "Modeling and simulation of the autonomous underwater vehicle, Autolycus," Master's thesis, MIT, 1999.

[19] S. F. Hoerner, *Fluid Dynamic Drag: Practical Information on Aerodynamic Drag and Hydrodynamic Resistance*. Hoerner Fluid Dynamics, 1965.

[20] T. Perez, *Ship Motion Control: Course Keeping and Roll Stabilisation Using Rudder and Fins*. Springer London, 2006.

[21] J. J. Craig, *Introduction to Robotics: Mechanics and Control*. Pearson Prentice Hall, 2005.

[22] M. J. Lighthill, "Large-amplitude elongated-body theory of fish locomotion," *Proceedings of the Royal Society of London. Series B. Biological Sciences*, vol. 179, no. 1055, pp. 125–138, 1971.

[23] J. J. Videler, *Fish Swimming*. Springer Dordrecht, 1993.